Vitrification, Devitrification, and Dielectric Relaxations During the Non-Isothermal Curing of Diepoxy-Cycloaliphatic Diamine

S. Montserrat, F. Roman, P. Colomer

Departament de Màquines i Motors Tèrmics, Universitat Politècnica de Catalunya, 08222 Terrassa, Spain

Received 7 November 2005; accepted 12 February 2006
DOI 10.1002/app.24295
Published online in Wiley InterScience (www.interscience.wiley.com).

ABSTRACT: The curing of an epoxy resin based on diglycidyl ether of bisphenol A (DGEBA) with a diamine based on 4,4′-diamino-3,3′-dimethyldicyclohexylmethane (3DCM) was analyzed by dielectric relaxation spectroscopy (DRS) between −100 and 220°C, at heating rates ranging from 0.1 to 2 K min^{-1}. The permittivity, ε', and the loss factor, ε'', were measured by DRS in the frequency range between 1 and 100 kHz. The dielectric relaxations were correlated with the relaxations observed previously by temperature modulated differential scanning calorimetry (TMDSC) at the same heating rates and in modulation conditions of amplitude 0.2 K and a period of 60 s, which is equivalent to a measuring frequency of 16.7 mHz. The dielectric measurements showed three frequency-dependent dipolar relaxations and one ionic relaxation, which was independent of the frequency. The dipolar relaxations were associated with the glass transition of the unreacted system and the vitrification and the devitrification processes of the system during the crosslinking reaction, and the ionic relaxation was associated with the beginning of the crosslinking reaction. © 2006 Wiley Periodicals, Inc. J Appl Polym Sci 102: 558–563, 2006

Key words: thermosets; crosslinking; glass transition; dielectric properties; temperature modulated differential scanning calorimetry

INTRODUCTION

The vitrification of a reacting system is a phenomenon related to the freeze-in of the motions of the molecular segments that can be studied by conventional DSC.[1,2] When the glass transition temperature (T_g) measured by DSC, also called thermal T_g, which is dependent on the cooling rate, equals the actual temperature, the system vitrifies and the progress of the reaction is collapsed. At this point the kinetics of the reaction changes from a chemically controlled regime to a diffusion-controlled regime.[3,4] This takes place only when the curing temperature is lower than the maximum glass transition temperature of the system, $T_{g\infty}$. The vitrification process is also observed in a system submitted to a constant heating rate when the T_g of the system equals the actual reaction temperature. However, this takes place only at a sufficiently low heating rate. In addition, as the actual temperature is continually increasing, the T_g of the system again becomes lower than this temperature and the system devitrifies.

The relaxation processes associated with these phenomena have been extensively studied using dynamic thermal analysis techniques such as temperature modulated differential scanning calorimetry (TMDSC),[5–10] and by other dynamic techniques such as torsional braid analysis.[11,12]

The molecular dynamics of the reaction of an epoxy crosslinked with an amine has been studied by dielectric relaxation spectroscopy (DRS) in a wide range of measuring frequencies. The conductive and dipolar response of an epoxy-amine system has been extensively studied in isothermal regime. For a brief reference we might cite the review by Johari[13] and the work of Tombari et al.,[14] Williams and coworkers[15,16] and several other authors.[17–21] Under isothermal conditions, a peak in ε'' appears, which tends to shift to higher reaction times as the measuring frequency decreases, due to the increase in the dipolar relaxation time as the reaction progresses. This frequency-dependent peak is attributed to the dipolar relaxation associated with the vitrification of the system.[21]

In the case of the nonisothermal curing of a thermoset, the molecular dynamics of the reacting system shows a more complex behavior. The increase in the crosslinking density as the reaction progresses leads to an increase in the characteristic relaxation time of the molecular segments, τ_0. Furthermore, the continuous heating of the system induces an increase in the thermal energy, which is translated into a decrease in the

Correspondence to: S. Montserrat (montserrat@mmt.upc.edu).
Contract grant sponsor: CICYT; contract grant numbers: 2000–1002-C02–01, 2004–04165-C02–01.

viscosity of the system and generates a decrease in τ_0. As pointed out by other authors,[22–25] the resulting effect is that during the nonisothermal curing of thermosets the progress of the reaction and the increase in thermal energy have competitive effects on the τ_0.

In the present study, these two competitive effects are analyzed in the relaxations observed in the dielectric measurements during the curing of an epoxy-diamine system at different heating rates. These relaxations are correlated with the phenomena of vitrification and devitrification observed in the same system using TMDSC, the results of which were shown in a previous paper.[10]

EXPERIMENTAL

Materials

The resin was an epoxy based on diglycidyl ether of bisphenol A (DGEBA) (Araldite LY564 from CIBA Speciality Chemicals), which was cured by a diamine based on 3,3′-dimethyl-4,4′-diaminodicyclohexylmethane (3DCM) (HY 2954 from CIBA Speciality Chemicals). The epoxy equivalent of the resin was 170 g equiv^{-1}. The preparation of the samples was performed as described elsewhere.[10]

Dielectric measurements

A DEA 2970 dynamic electric analyzer from TA Instruments was used to measure, in real time, the dielectric permittivity (ε') and the dielectric loss factor (ε'') of the epoxy samples cured at different frequencies. The complex dielectric constant, ε^*, may be expressed by a general equation

$$\varepsilon^* = \varepsilon' - i\varepsilon'' \tag{1}$$

where ε' is the permittivity and ε'' is the loss factor. For epoxy resins with a low ionic concentration, ε' is determined only by the dipolar orientation polarization and ε'' is determined by both the ionic conduction and the dipolar reorientation[13]

$$\varepsilon'(\omega, T_c, t_c) = \varepsilon'_d(\omega, T_c, t_c) \tag{2}$$

and

$$\varepsilon''(\omega, T_c, t_c) = \varepsilon''_d(\omega, T_c, t_c) + \varepsilon''_i(T_c, t_c) \tag{3}$$

where ε''_d is the dipolar contribution to ε'', ε''_i represents the contribution of the dc conductivity to ε'', ω is the angular frequency ($\omega = 2\pi f$) of the electrical field applied, f is the measuring frequency, and T_c and t_c are the curing temperature and time, respectively. The conductivity is related to the loss factor by the relation $\sigma = \varepsilon'' e_0 \omega$, where e_0 is the permittivity (8.85 pF m^{-1}) of free space. This relation allows the conductivity to be expressed by the contribution of the direct current component σ_{dc}, which is attributed to the pure conductive process, and the alternative current component σ_{ac}, which is related to the dipolar relaxation:

$$\sigma(\omega, T_c, t_c)) = \sigma_{dc}(T_c, t_c) + \sigma_{ac}(\omega, T_c, t_c) \tag{4}$$

Alternatively, ε^* may be expressed in the following form:

$$\varepsilon^*(\omega, T_c, t_c) = \varepsilon'_d(\omega, T_c, t_c) - i[\sigma_{dc}(T_c, t_c) + \sigma_{ac}(\omega, T_c, t_c)]/\omega e_0 \tag{5}$$

Dielectric measurements were performed using a ceramic single-surface cell of 20 × 25 mm^2 based on a coplanar inter-digitated comb-like electrode design. The values of ε' and ε'' were calculated from the resulting current and the induced phase angle shift. The interval of data sampling was 5 s per point. The mixture of epoxy-amine was spread on the electrode surface, covering the entire inter-digitated area. The nonisothermal curing measurements were performed at temperatures from −100 to 220°C in a nitrogen atmosphere with a gas flow of 500 mL min^{-1}. The heating rates were between 0.1 and 2 K min^{-1}. The dielectric permittivity and the dielectric loss factor were measured at frequencies in the interval of 1 to 100 kHz. The time taken to scan the different frequencies was 1.2 min.

RESULTS AND DISCUSSION

The dielectric analysis was performed from the unreacted mixture of DGEBA–3DCM at a temperature of −100°C to a temperature of 220°C, at which the system can be considered fully cured. The results obtained for the permittivity ε', the loss factor ε'', and conductivity σ at a heating rate of 0.5 K min^{-1} at frequencies between 10 and 100 kHz are shown in Figure 1. The DRS results can be compared to those of a previous calorimetric study of this system performed by TMDSC.[10] Figure 2(a) shows the total heat flow obtained at 0.5 K min^{-1}, which is the same signal that we would obtain by conventional DSC at the same heating rate[26]; the degree of conversion of the system during the curing is also shown in Figure 2(a).

The analysis of the dielectric results can be divided into two regions. Region I corresponds to the unreacted system from the glassy state to the liquid state close to the beginning of the crosslinking reaction, as is shown from −60 to ~45°C in the heat flow curve in Figure 2(a). Region II corresponds to the crosslinking reaction of the system, from about 45°C to the end of the reaction at 210°C in Figure 2(a).

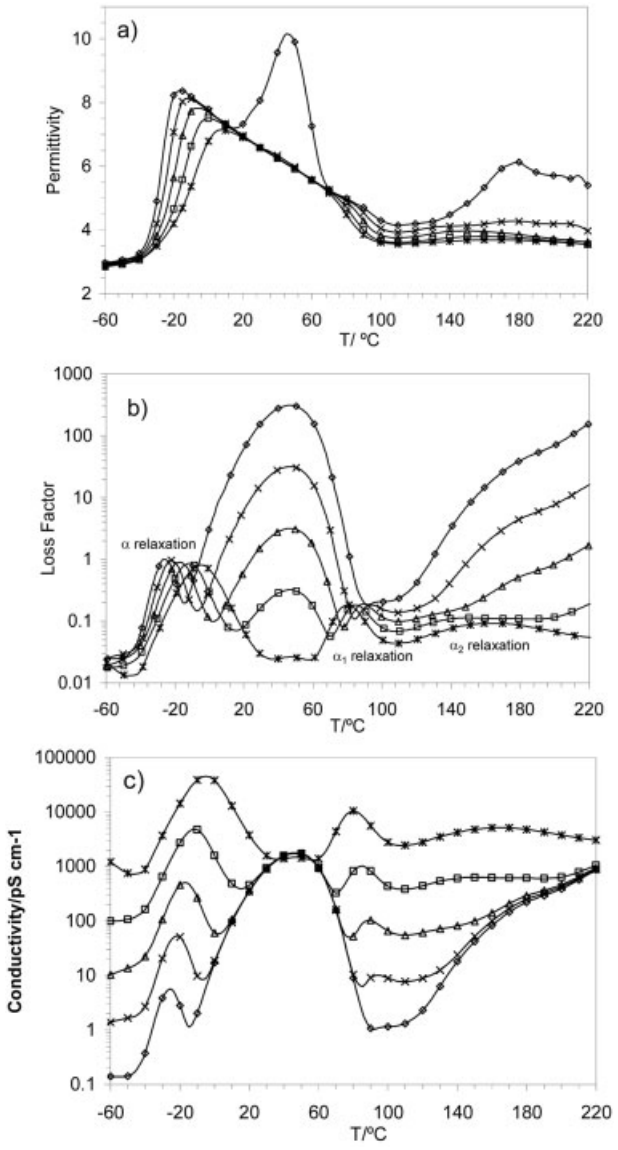

Figure 1 Variation of the permittivity ε' (a), loss factor ε'' (b), and conductivity σ (c) during the curing of the DGEBA–3DCM system at a heating rate of 0.5 K min^{-1}, and frequencies measured in the range between 10 Hz and 100 kHz: 10Hz (◇), 100 Hz (×), 1 kHz (Δ), 10 kHz (□), and 100 kHz (∗).

In Region I, the dielectric properties ε', ε'', and σ change in the absence of a crosslinking reaction as the temperature is increased. In the interval between −60 and −50°C, the permittivity shows a small variation, and takes a value close to the high-frequency limiting permittivity ε_∞. Thereafter, ε' gradually increases with temperature to reach the low frequency limiting permittivity ε_s, which is frequency-independent in the temperature interval between 10 and 60°C. However, at frequencies lower than 100 Hz an abrupt increase of the measured permittivity is observed as a result of electrode polarization. According to Sheppard and Senturia,[27] the electrode begins to polarize once the frequency is lowered such that tan $\delta(=\varepsilon''/\varepsilon')$ becomes significantly greater than unity. In our epoxy-diamine system the aforementioned condition is fulfilled, since tan δ is ~40 for 10 Hz ($\varepsilon'' \approx 400$ and $\varepsilon' \approx 10$) and ~30 for 1 Hz ($\varepsilon'' \approx 3000$ and $\varepsilon' \approx 100$), though the values for 1 Hz are not shown in Figure 1.

The loss factor shows a well-defined peak, which shifts to higher temperatures as the frequency increases. The nature of this peak is dipolar and corresponds to the α relaxation associated with the glass transition region, which is observed between −50 and −35°C in the heat flow signal shown in Figure 2(a). An average relaxation time $<\tau_0>$ can be calculated at the temperature of the maximum $\langle\tau_0\rangle = (2\pi f)^{-1}$ that decreases as the temperature increases. This behavior is similar to that observed in the devitrification phenomenon of DGEBA without hardener.[27] As was observed in other epoxy-amine systems, such as the DGEBA and *p*-aminodicyclohexylmethane (PACM),[24] ε'' reaches a minimum when ε' approaches the low frequency limiting permittivity ε_s. When the temperature is increased, ε'' tends to increase as a consequence of the contribution of the dc conductivity, which also increases when the system is heated. The magnitude of the increase of ε'' with increase in temperature decreases as the frequency rises, becoming practically

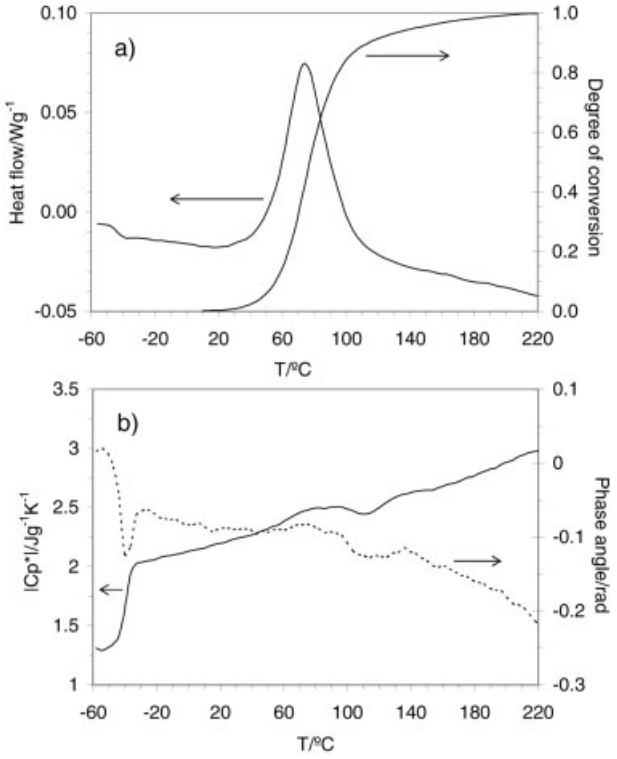

Figure 2 Heat flow and degree of conversion (a) and modulus of the complex heat capacity (C_p^*) and phase angle (b) during the curing of the DGEBA–3DCM system, which were obtained by temperature modulated differential scanning calorimetry at an average heating rate of 0.5 K min^{-1}, an amplitude of 0.2 K, and a modulation period of 60 s.

negligible at a frequency of 100 kHz, as shown in Figure 1(b). Additionally, the increase in the conductivity is frequency-independent, as shown in Figure 1(c).

Region II includes the relaxations which occur in the reacting system. At the beginning of the crosslinking reaction, both ε'' and σ show a maximum in practically the whole range of frequencies, except for the frequency 100 kHz. For the conditions shown in Figures 1(b) and 1(c), this maximum takes place at 46°C, which corresponds to a practically negligible degree of reaction ($\alpha \approx 0.04$), as may be seen in Figure 2(a). As the crosslinking progresses through a chemically controlled kinetics, the conductivity and ε'' of the system decrease with the increase in temperature. Thereafter, a peak in ε'' is observed for practically all the measuring frequencies. This peak, which is named α_1 relaxation, is frequency-dependent and can be considered to have a dipolar nature. The maximum of this peak tends to shift to higher temperatures as the frequency decreases. This means that $\langle \tau_0 \rangle$ tends to increase with the increase in temperature and correspondingly to an increase in the degree of conversion. At the same time, a gradual decrease, which is also frequency-dependent, is observed in ε'. It is also observed that the decrease in ε' in the reacting system takes place in a reverse order to that in the unreacted system. These observations suggest that the α_1 relaxation may be associated with a vitrification phenomenon, which was also detected in the same system due to an abrupt decrease in the heat capacity shown in the TMDSC measurements (Fig. 6, Ref. 10).

According to other authors,[5–7,9,21,28] TMDSC measurements have proven to be a suitable technique for studying the vitrification of thermosets. In particular, in the DGEBA–3DCM system, the measurement of the dynamic T_g, which is frequency-dependent, obtained by the C_p^* signal at a modulation period of 60 s (equivalent to a measuring frequency of 16.7 mHz), gives a value for the vitrification time (in isothermal measurements) that is very close to that measured by conventional DSC.[28] This property is common to other epoxy-amine systems that follow a step reaction, but it cannot be generalized to other types of reacting systems, such as the chain reaction that occurs in epoxy-anhydride systems.[29] Similarly, TMDSC can be used to determine the region of vitrification and further devitrification, which occurs during the non isothermal crosslinking reaction at a sufficiently low heating rate.[6,10] These two phenomena are shown in Figure 2(b) in the modulus of the complex heat capacity C_p^* and the phase angle δ signals obtained by TMDSC at an underlying heating rate of 0.5 K min^{-1}, an amplitude of 0.2 K, and a modulation period of 60 s. In the range between 97 and 108°C a decay of C_p^* is observed, whose midpoint value of 103°C is assigned to the midpoint of the vitrification process. The value of the vitrification temperature obtained by TMDSC is higher than the values reached by the peak temperature of ε'', which are 94 and 80°C at a frequency of 100 Hz and 100 kHz, respectively, because of the lower frequency of the TMDSC experiments, which is 16.7 mHz.

When the temperature is increased, a wide and flat peak is observed in the loss factor [Fig. 1(b)]. This peak is better shown at high frequencies (between 10 and 100 kHz) than at low frequencies because of the greater contribution of the conduction at frequencies lower than 10 kHz, as shown in Figure 1(c). This peak, which is referred to as the α_2 relaxation, is also frequency-dependent: an increase in the frequency shifts the maximum to higher temperatures. Taking into account the characteristic relaxation time $\langle \tau_0 \rangle$ of this α_2 peak, an increase in the temperature corresponds to a decrease in $\langle \tau_0 \rangle$, which indicates that the effect of the thermal energy is predominant on the extent of cure. This peak, which can be considered to have a dipolar nature, is associated with a devitrification phenomenon. The devitrification process for the DGEBA–3DCM system can be observed as an increase in the C_p^* signal obtained by TMDSC between 113 and 130°C, with a midpoint of 121°C, as shown in Figure 2(b). During the vitrification process the reacting system becomes freeze-in and the kinetics is diffusion-controlled, but as the temperature increases the system undergoes a devitrification process, which allows the chemical reaction to continue. Nevertheless, because of the high value of the extent of cure, the reaction rate is much slower than before the vitrification phenomenon. This effect can be observed in the slope of the curve of the degree of conversion shown in Figure 2(a). At a heating rate of 0.5 K min^{-1}, the α_2 relaxation takes place at 146°C for a frequency of 3 kHz and at 166°C for a frequency of 100 kHz, and these values correspond to an interval of the degree of conversion between 0.95 and 0.96. The full conversion is practically achieved at 220°C. A second scan of the fully cured system, performed at 2 K min^{-1}, shows a dipolar relaxation at about 179°C for 10 kHz and 188°C for 100 kHz, which is associated with the maximum glass transition of the fully cured epoxy (Fig. 3). At frequencies lower than 10 kHz there are additional conduction effects superposed on this relaxation. Furthermore, Figure 3 shows sub-T_g relaxations, such as the γ and β relaxations, which have also been identified in other epoxy-diamine systems.[30] At low frequencies, such as 1 Hz, the γ and β relaxations are shown as two wide peaks at temperatures between −100°C and 0°C and between 10 and 70°C, respectively. As the frequency increases, these relaxation peaks tend to shift to higher temperatures and finally, at frequencies higher than 10 kHz, they tend to overlap.

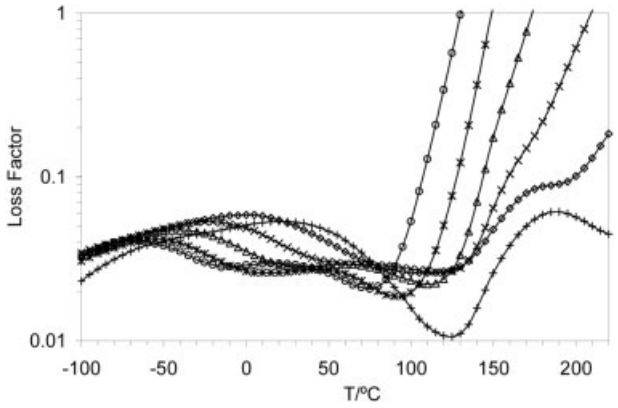

Figure 3 Variation of the loss factor in the fully cured epoxy system at a heating rate of 2 K min^{-1} and the following frequencies: 1 Hz (○), 10 Hz (∗), 100 Hz (Δ), 1 kHz (×), 10 kHz (◇), and 100 kHz (+).

Figure 1(b) shows that the magnitude of the α_1 relaxation is much smaller than that of the α relaxation in the unreacted system, which may be attributed to the crosslinks present in the reacting system. In addition, the lower the heating rate, the higher the magnitude of the α_1 relaxation, as shown in Figure 4. A similar effect was observed during the vitrification in the variation of the heat capacity measured by TMDSC (Fig. 6, Ref. 10).

In Region II, two competitive effects are observed when the temperature is increased: an increase in the crosslinking density that leads to an increase in $<\tau_0>$, and an increase in the thermal energy that leads to a decrease in $<\tau_0>$. Both effects are shown for different heating rates in Figure 5, where log $<\tau_0>$ is plotted against the temperature for both relaxations: α_1 associated with the vitrification and α_2 associated with the devitrification, at different heating rates. During the vitrification, $<\tau_0>$ increases with the increase in temperature, indicating that the increase in the degree of reaction dominates $<\tau_0>$, while $<\tau_0>$ decreases with the increase in temperature during the devitrification, indicating that the thermal energy dominates $<\tau_0>$. At a heating rate of 2 K min^{-1}, the α_1 relaxation was clearly observed but the relaxation α_2 appears as a shoulder close to α_1, which does not allow the peak temperature to be determined. These results seem to indicate that there is a temperature for which the tendency of $<\tau_0>$ to increase reverses to the opposite tendency. The values of vitrification previously obtained by TMDSC[10] are also plotted in Figure 5, showing a good correlation with those obtained by DRS. Nevertheless, the TMDSC values of devitrification are practically independent of the heating rate and the correlation with the values of α_2 is not good. At a heating rate of 1 K min^{-1}, neither vitrification nor devitrification was observed by TMDSC (Fig. 6, Ref.10).

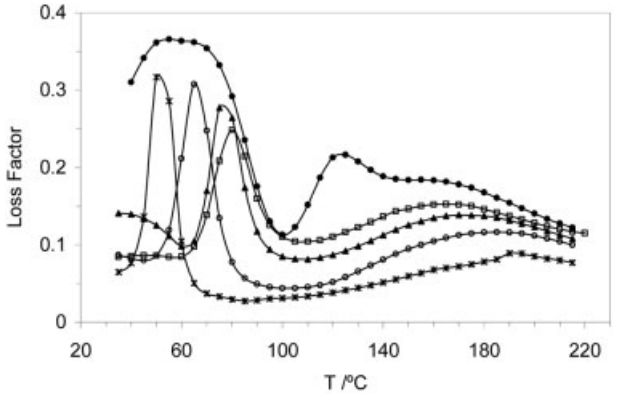

Figure 4 Variation of the loss factor during the curing of the DGEBA–3DCM system at a frequency of 100 kHz and the indicated heating rates in K min^{-1}: 0.1 (∗), 0.25 (○), 0.4 (Δ), 0.5 (□), and 2 (●).

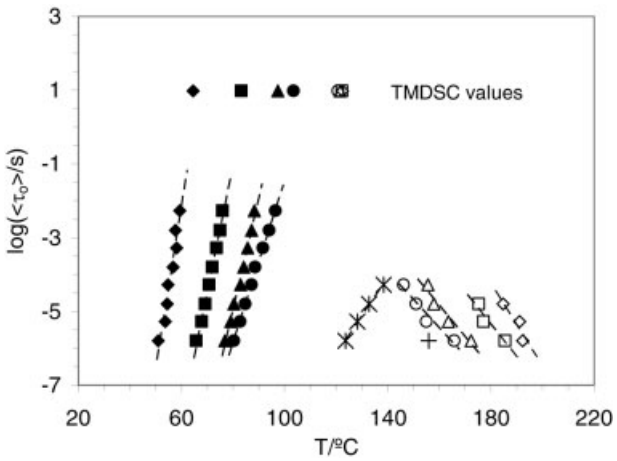

Figure 5 Variation of the characteristic relaxation time $<\tau_0>$ at the peak temperature of the α_1 relaxation and α_2 relaxation at the indicated heating rates in K min^{-1}: α_1 relaxation [0.1 (♦), 0.25 (■), 0.4 (▲), 0.5 (●) and 2 (∗)] and α_2 relaxation [0.1 (◇), 0.25 (□), 0.4 (Δ), 0.5 (○) and 2 (+)]. The dashed lines are a guide for the eye. The symbols shown in the upper part of the diagram, for a $\log\langle\tau_0\rangle$ = 0.98 s, correspond to the values previously obtained by TMDSC[10] at the same heating rates between 0.1 and 0.5 K min^{-1}.

The temperature and the time at which the α_1 and α_2 relaxations were observed were plotted in a continuous heating transformation (CHT) cure diagram, as shown in Figure 6. By connecting the points obtained at different heating rates, one can obtain the α_1 relaxation line associated with the vitrification process (vitrification line in Fig. 6) and the α_2 relaxation line associated with the devitrification process (devitrification line in Fig. 6) for each measuring frequency. For reasons of clarity, the dielectric values for only two measuring frequencies have been plotted (10 and 100 kHz) in the diagram. The α relaxation associated with the glass transition of the unreacted system T_{g0} is also

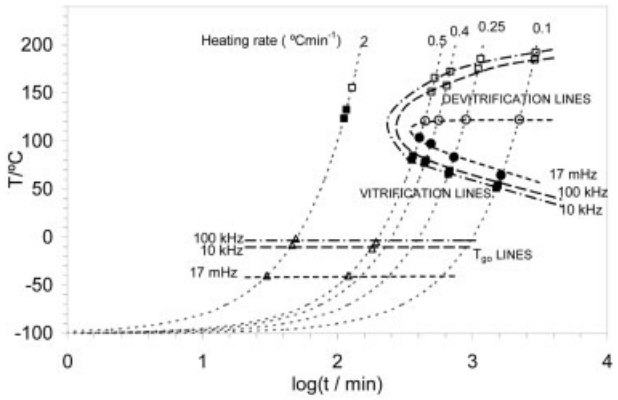

Figure 6 Continuous heating transformation cure diagram of the DGEBA–3DCM system. The dotted lines show the indicated heating rate. The filled symbols (■) and open symbols (□) correspond to the α_1 relaxation (vitrification) and α_2 relaxation (devitrification), respectively, at 10 and 100 kHz. The α relaxation associated with the glass transition of the unreacted system T_{g0} is also indicated (Δ). The dashed lines that connect each type of relaxation serve as a guide for the eye. The data at 17 mHz correspond to the TMDSC measurements, which were obtained in a previous research work.[10]

indicated in Figure 6 (T_{g0} line). As stated earlier, the DRS results obtained for the vitrification phenomenon correlate very well with the TMDSC results obtained in a previous paper.[10] Nevertheless, the results for the relaxation associated with the devitrification seem to be more dependent on the heating rate than the results obtained by TMDSC, in which the devitrification temperature is practically independent of the heating rate.

CONCLUSIONS

The relaxations that appear during the nonisothermal curing of the DGEBA–3DCM system were analyzed by DRS in a range of frequencies between 1 Hz and 100 kHz and compared with the thermal relaxation previously observed in the same system by TMDSC at heating rates lower than 2 and 0.5°C min^{-1}, respectively. The three frequency-dependent relaxations observed by DRS are associated with the devitrification (α relaxation) of the unreacted system and with further vitrification (α_1 relaxation) and devitrification (α_2 relaxation), which occur during the crosslinking reaction. The increase in the characteristic relaxation time $<t_0>$ with the temperature during the α_1 relaxation indicates that the degree of conversion dominates $<t_0>$, while the decrease in $<t_0>$ with the temperature during the α_2 relaxation indicates that the thermal energy dominates this parameter. This behavior of $<t_0>$ seems to indicate that there is a temperature for which the variation in $<t_0>$ with temperature is reversed.

A continuous heating transformation cure diagram can be built by the temperature–time values of the three dipolar relaxations. The diagram shows the lines of the α_1 and α_2 relaxations associated with the vitrification and the devitrification processes, respectively, and the line of the α relaxation associated with the glass transition of the unreacted system for different measuring frequencies.

The authors are grateful to CIBA Speciality Chemicals for supplying the epoxy and the hardener.

References

1. Prime, R. B. In Thermal Characterization of Polymeric Materials; Turi, E. A., Ed.; Academic Press: San Diego, 1997; Vol. 2, Chapter 6.
2. Montserrat, S. J Appl Polym Sci 1992, 44, 545.
3. Havlicek, I.; Dusek, K. In Crosslinked Epoxies; Sedlácek, B.; Kahovec, J., Eds.; Walter de Gruyter: Berlin, 1987; p 417.
4. Gillham, J. K. Polym Eng Sci 1986, 26, 1429.
5. Van Assche, G.; Van Hemelrijck, A.; Rahier, H.; Van Mele, B. Thermochim Acta 1996, 286, 209.
6. Van Assche, G.; Van Hemelrijck, A.; Rahier, H.; Van Mele, B. Thermochim Acta 1997, 304/305, 317.
7. Swier, S.; Van Assche, G.; Van Hemelrijck, A.; Rahier, H.; Verdonck, E.; Van Mele, B. J Therm Anal 1998, 54, 585.
8. Flammersheim, H. J.; Opfermann, J. Thermochim Acta 1999, 337, 141.
9. Montserrat, S.; Cima, I. Thermochim Acta 1999, 330, 189.
10. Montserrat, S.; Martín, J. G. Thermochim Acta 2002, 388, 343.
11. Wisanrakkit, G.; Gillham, J. K.; Enns, J. B. J Appl Polym Sci 1990, 41, 1895.
12. Wisanrakkit, G.; Gillham, J. K. J Appl Polym Sci 1992, 42, 2453.
13. Johari, G. P. In Chemistry and Technology of Epoxy Resins; Ellis, B., Ed.; Chapman & Hall: Glasgow, 1996; Chapter 6.
14. Tombari, E.; Ferrari, C.; Salvetti, G.; Johari, G. P. Phys Chem Chem Phys 1999, 1, 1965.
15. Fournier, J.; Williams, G.; Duch, C.; Aldridge, G. A. Macromolecules 1996, 29, 7097.
16. Williams, G.; Smith, I. K.; Aldridge, G. A.; Holmes, P. A.; Varma, S. Polymer 2001, 42, 3533.
17. Sheppard, N. F.; Senturia, S. D. Polym Eng Sci 1986, 26, 354.
18. Bartolomeo, P.; Chailan, J. F.; Vernet, J. L. Polymer 2001, 42, 4385.
19. Alig, I.; Jenninge, W.; Junker, M.; de Graaf, L. A. J Macromol Sci Phys 1996, B35, 563.
20. Bonnet, A.; Pascault, P. P.; Sautereau, H.; Rogozinski, J.; Kransbuehl, D. Macromolecules 2000, 33, 3833.
21. Montserrat, S.; Roman, F.; Colomer, P. Polymer 2003, 44, 101.
22. Parthum, M. G.; Johari, G. P. Macromolecules 1992, 25, 3149.
23. Wasylyshyn, D. A.; Johari, G. P.; Tombari, E.; Salvetti, G. Chem Phys 1997, 223, 313.
24. Tombari, E.; Salvetti, G.; Johari, G. P. J Chem Phys 2000, 113, 6957.
25. Cardelli, C.; Tombari, E.; Johari, G. P. J Phys Chem B 2001, 105, 11035.
26. Hutchinson, J. M.; Montserrat, S. Thermochim Acta 1997, 304/305, 257.
27. Sheppard, N. F.; Senturia, S. D. J Polym Sci Part B: Polym Phys 1989, 27, 753.
28. Montserrat, S.; Martín, J. G. J Appl Polym Sci 2002, 85, 1263.
29. Montserrat, S.; Pla, X. Polym Int 2004, 53, 326.
30. Mangion, M. B. M.; Johari, G. P. J Polym Sci Part B: Polym Phys 1990, 28, 71.